A Unified Micromechanical Model for the Mechanical Properties of Two Constituent Composite Materials. Part V: Laminate Strength

ZHENG MING HUANG[1]
Department of Mechanics
Huazhong University of Science & Technology
Wuhan, Hubei 430074
People's Republic of China

ABSTRACT: This series of papers reports a new, general, and unified micromechanical model for estimating the three-dimensional mechanical properties of a composite made from two constituent materials, i.e., continuous fibers and matrix. Various mechanical properties, i.e., elastic, elasto-plastic, strength, and rubber-elastic properties, of unidirectional laminae made using different constituent materials have been simulated in Parts I–IV. The present paper addresses the problem of failure analysis and strength prediction of laminated composites consisting of different unidirectional laminae. By using the classical laminate theory, the stress shared by each lamina ply in the laminate can be determined, and the lamina analysis theory reported previously can be applied. The progressive failure process in the laminate is treated through stiffness reduction. As soon as one ply fails, it has no further contribution to the overall instantaneous stiffness matrix of the laminate, and the total strength of the laminate corresponds to a load level at which all the plies have failed. A generalized maximum normal stress criterion, which accounts for equibiaxial and equitriaxial tensions, is used to detect the lamina tensile failure, whereas the lamina compressive failure is controlled using a criterion similar to the original maximum normal stress criterion. The present modeling procedure has been applied to four different angle-ply laminates subjected to various biaxial load conditions. Favorable correlation between predictions and available test data has been found.

KEY WORDS: fibrous composites, laminated composites, mechanical property, progressive failure process, failure criteria, tensile strength, compressive strength, modeling approach, micromechanical model, unified model.

[1]Present address: Department of Mechanical & Production Engineering, National University of Singapore, 10 Kent Ridge Crescent, Singapore 119260.

0892-7057/00/03 0190–17 $10.00/0

1. INTRODUCTION

THE HIGH SPECIFIC strength and stiffness of advanced fibrous composites make these materials attractive candidates for many critical applications. Extensive acceptance and utilization of structures fabricated from composite materials requires comprehensive understanding of their strength behavior under complicated stress states. Most structural composites in engineering applications consist of multidirectional plies of laminates for structural integrity. In reality, however, the failure mechanisms in laminates are much more complicated than those involved in a unidirectional lamina. The virtually limitless combinations of ply materials, ply orientations, and ply stacking sequences offered by laminated construction considerably enhance the design flexibility inherent in composite structures and thus cause difficulty in laminate failure analyses. Most laminates display a progressive failure process when subjected to applied external loads. In general, the failure of the laminated composite in any one ply does not imply failure of the other plies, nor does it mean the rupture of the whole laminate. Therefore, the ability to predict failure strength of laminates is a key aspect in the successful design of an engineering composite structure.

A great deal of effort has been made over the past several decades to develop a reliable methodology to analyze the failure strength of composite laminates. Surveys of the available failure theories can be found in References [5]–[11], among others. Most of these theories have been developed phenomenologically, employing overall strength behavior of the laminae in the laminate as input information. As has been pointed out in the third paper of this series [3], extensive experiments on the laminae, probably including biaxial tests, are necessary to determine the strength coefficients involved in the phenomenological failure theories. Such experiments may be difficult or expensive in some situations. The situation becomes even worse if a certain ply in the laminate has a different fiber volume fraction. Furthermore, the measured strength parameters of the laminae can still be insufficient for accurate prediction of the failure strength of the composite laminates. It has been recognized that non-linear response is distinct in laminated composites. The non-linearity of the stress-strain response of a laminate results mainly from two sources: (1) material non-linearity and (2) progressive failure in the laminate. While a unidirectional lamina generally reveals a linear stress-strain curve to a longitudinal load, the angle-plied lamina in the laminate may display a non-linear response even under a uniaxial load applied to the laminate. This is because the lamina in the laminate may be subjected to the resulting transverse and shear loads. Hence, the material non-linearity should be incorporated in an accurate failure theory for laminated composites. Nevertheless, it is difficult to account for the material non-linearity with a phenomenological failure theory [7]. As such, a micromechanics theory, which recognizes the non-linear stress-strain behavior of the constituent fiber and matrix materials and identifies the progressive failure process

in the laminate, would show more promise for the prediction of the laminate failure strength.

In References [1], [2], and [4], the author developed a unified yet user-friendly micromechanical model, which can predict the entire stress-strain response of a composite lamina made from any two constituent materials subjected to an arbitrary load condition. The three-dimensional instantaneous stiffness matrix of the lamina at each load level is expressed in terms of those of the constituent fiber and matrix materials, regardless of whether these constituents are linearly elastic, elasto-plastic, or rubber-elastic. The material non-linearity of a lamina has been completely characterized with this unified model. On the other hand, the classical laminate theory can distribute an overall applied load on the laminate to each lamina ply based on information about the lamina's instantaneous stiffness matrix. Combining the unified model with the classical laminate theory, a micromechanical modeling approach to the failure strength of laminated composites is established. The strength theory developed in Reference [3] is generalized in the present study to determine whether any lamina ply has failed or not. Both tensile and compressive strengths of the lamina are defined. For the compressive strength, a similar criterion as in Reference [3] is applied. For the tensile strength, however, a generalized maximum normal stress criterion is adopted in order that an equibiaxial or equitriaxial tension can be tailored. Once a lamina ply fails, it makes no further contribution to the overall instantaneous stiffness matrix of the laminate. In this way, the progressive failure process in the laminate is addressed. The modeling approach has been applied to several angle-ply laminates subjected to multiaxial stress states. The predicted failure envelopes are in satisfactory agreement with available experimental data for all the cases considered.

2. LAMINA ANALYSIS

In this section, the stress analysis of a unidirectional fibrous lamina presented in References [1] and [2] is briefly summarized for convenience of description. Terms and notations used are defined in References [1] and [2]. Criteria to detect tensile as well as compressive failures of the constituent fiber and matrix materials are also given. Based on these criteria, the lamina tensile and compressive strengths can be estimated.

2.1. Stress Analysis

Let (x_1, x_2, x_3) be the material coordinate system of the lamina with the x_1-axis along the fiber direction. Casting the overall applied load in an incremental form, the stress increments in the fiber and matrix phases of the lamina, and the lamina's instantaneous compliance matrix are, respectively, given by [1,2]

$$\{d\sigma_i^f\} = (V_f[I] + V_m[A_{ij}])^{-1}\{d\sigma_j\} \tag{1}$$

$$\{d\sigma_i^m\} = [A_{ij}](V_f[I] + V_m[A_{ij}])^{-1}\{d\sigma_j\} \tag{2}$$

and

$$[S_{ij}] = (V_f[S_{ij}^f] + V_m[S_{ij}^m][A_{ij}])(V_f[I] + V_m[A_{ij}])^{-1} \tag{3}$$

where the instantaneous compliance matrices of the constituents, $[S_{ij}^f]$, $[S_{ij}^m]$, are given in Reference [2] for elasto-plastic materials, or in Reference [4] for rubber-elastic materials. The bridging matrix, $[A_{ij}]$, is defined as

$$[A_{ij}] = \begin{bmatrix} a_{11} & a_{12} & a_{13} & a_{14} & a_{15} & a_{16} \\ & a_{22} & a_{23} & a_{24} & a_{25} & a_{26} \\ & & a_{33} & a_{34} & a_{35} & a_{36} \\ & & & a_{44} & a_{45} & a_{46} \\ & & & & a_{55} & a_{56} \\ 0 & & & & & a_{66} \end{bmatrix} \tag{4}$$

The elements on the diagonal of Equation (4) read [1,2,4]

$$a_{11} = E_m/E_f \tag{5.1}$$

$$a_{22} = a_{33} = a_{44} = 0.5(1 + E_m/E_f) \tag{5.2}$$

$$a_{55} = a_{66} = 0.5\left[1 + \frac{E_m(1-\nu_f)}{E_f(1-\nu_m)}\right] \tag{5.3}$$

where E_f, E_m, ν_f, and ν_m are the load-dependent (tangential) moduli and the Poisson's ratios of the fiber and matrix, respectively. It is to be noted that the expression for a_{44} given here is a concise form of that originally presented in Reference [2]. The off-diagonal elements of Equation (4) are determined by substituting Equation (4) into Equation (3) and by requiring the resulting overall compliance matrix, $[S_{ij}]$, to be symmetric, i.e.,

$$S_{ji} = S_{ij} \text{ for all } i, j = 1,2,\ldots,6, \quad i \neq j \tag{6}$$

The total stresses in various material phases are simply updated through

$$[\sigma_{ij}]^{(n+1)} = [\sigma_{ij}]^{(n)} + [d\sigma_{ij}],\ [\sigma_{ij}^f]^{(n+1)} = [\sigma_{ij}^f]^{(n)} + [d\sigma_{ij}^f]$$
$$[\sigma_{ij}^m]^{(n+1)} = [\sigma_{ij}^m]^{(n)} + [d\sigma_{ij}^m] \tag{7}$$

2.2. Failure Criteria

As the stress states in the constituent materials are explicitly known, a failure criterion is intuitively applied to the constituent materials. The lamina strength is assumed when any constituent material fails. In Reference [3], the maximum normal stress criterion of isotropic materials was used to determine the lamina's tensile strength. This criterion is efficient when the three principal stresses of the material differ from each other significantly. If, however, two or three of them become equal, the accuracy of this criterion is certainly questionable. Otherwise, a material would be able to sustain the same amount of equibiaxial or equitriaxial tension as it does uniaxial tension. Phenomenologically, this might be impossible. The load-carrying capacity of an isotropic material when subjected to an equibiaxial or equitriaxial tension should decrease somewhat compared to uniaxial tension. Recognizing this fact, a generalized criterion to detect tensile failure of the material is expressed as

$$\sigma_{eq} \geq \sigma_u \tag{8.1}$$

where

$$\sigma_{eq} = \begin{cases} \sigma^1, & when\ \ \sigma^3 < 0 \\ [(\sigma^1)^q + (\sigma^2)^q]^{1/q}, & when\ \ \sigma^3 = 0 \\ [(\sigma^1)^q + (\sigma^2)^q + (\sigma^3)^q]^{1/q} & when\ \ \sigma^3 > 0, 1 < q \leq \infty \end{cases} \tag{8.2}$$

In the above, σ^1, σ^2, and σ^3 are the three principal stresses of the material with $\sigma^1 \geq \sigma^2 \geq \sigma^3$, and σ_u is the ultimate tensile strength of the material under a uniaxial load. The power-index q, a real number greater than 1, can be determined experimentally. It is seen that when the power-index $q = \infty$, Equation (8.1) together with (8.2) is equivalent to the maximum normal stress criterion. For this reason, the condition represented by Equations (8.1) and (8.2) is named as a generalized maximum normal stress criterion. In fact, the difference between the generalized and the original maximum normal stress criteria is distinct only when the second or the third principal stress of the material is close to its first principal stress. As will be shown subsequently, a proper choice of the power-index in Equation (8.2) should be $q > 2$. In this paper, $q = 3$ is used throughout.

In contrast to multiaxial tensions, an equitriaxial compression on an isotropic material can hardly cause it to fail. Hence, a criterion to govern the compressive failure of the material is simply given by

$$\sigma^3 \leq (-\sigma_{u,c}) \tag{9}$$

where $\sigma_{u,c}$ is the ultimate compressive strength of the material under a uniaxial load. It should be pointed out that no material buckling is assumed in the compression concerned herein. Further, the material parameters used in Equations (5.1)–(5.3) may be different under compression from those under tension.

3. LAMINATE ANALYSIS

Suppose that a laminated composite consists of a number of unidirectional laminae, stacked in different ply-angles. Each lamina can have different constituent materials and a different fiber volume fraction. A global coordinate system, (x, y, z), is assumed to have its origin on the middle surface of the laminate, with x and y being in the laminate plane and z along the thickness direction. Let the fiber direction of the kth lamina have an inclined ply-angle θ_k with the global x direction. According to the classical laminate theory, only the in-plane stress and strain increments, i.e., $\{d\sigma\}^G = \{d\sigma_{xx}, d\sigma_{yy}, d\sigma_{xy}\}^T$ and $\{d\epsilon\}^G = \{d\epsilon_{xx}, d\epsilon_{yy}, 2d\epsilon_{xy}\}^T$, are retained, where G refers to the global coordinate system. The out-of-plane strain increments are assumed to be zero, whereas the out-of-plane stress increments can be obtained once the in-plane strain increments are determined. The global in-plane strain increments of the laminate at a material point (x, y, z) are expressed as [12]

$$d\epsilon_{xx} = d\epsilon^0_{xx} + z d\kappa^0_{xx},\ d\epsilon_{yy} = d\epsilon^0_{yy} + z d\kappa^0_{yy},\ 2d\epsilon_{xy} = 2d\epsilon^0_{xy} + 2z d\kappa^0_{xy}$$

where

$$d\epsilon^0_{xx} = \frac{\partial(du^0)}{\partial x},\ d\epsilon^0_{yy} = \frac{\partial(dv^0)}{\partial y},\ d\epsilon^0_{xy} = \frac{1}{2}\left(\frac{\partial(du^0)}{\partial y} + \frac{\partial(dv^0)}{\partial x}\right) \tag{10.1}$$

and

$$d\kappa^0_{xx} = -\frac{\partial^2(dw^0)}{\partial x^2},\ d\kappa^0_{yy} = -\frac{\partial^2(dw^0)}{\partial y^2},\ d\kappa^0_{xy} = -\frac{\partial^2(dw^0)}{\partial x \partial y} \tag{10.2}$$

are the strain and the curvature increments of the middle surface, respectively. In the above, u^0, v^0, and w^0 are the displacement components of the middle surface of the laminate along the x-, y-, and z-directions, respectively. Suppose that the mate-

rial point is on the kth lamina ply of the laminate. The global stress increments at this point are obtained from

$$\{d\sigma\}^G = [C]_k^G \{d\epsilon\}^G = [(C_{ij}^G)_k]\{d\epsilon\}^G = ([T]_c)_k([S]_k)^{-1}([T]_c^T)_k\{d\epsilon\}^G \quad (11)$$

where $[S]_k$ is the compliance matrix (3×3) of the kth lamina in its local (material) coordinate system given by [see Equation (3)]

$$[S]_k = \begin{bmatrix} S_{11} & S_{12} & S_{16} \\ & S_{22} & S_{26} \\ symmetry & & S_{66} \end{bmatrix}_k$$

and

$$[T]_c = \begin{bmatrix} l_1^2 & l_2^2 & 2l_1l_2 \\ m_1^2 & m_2^2 & 2m_1m_2 \\ l_1m_1 & l_2m_2 & l_1m_2 + l_2m_1 \end{bmatrix} \quad (12)$$

is a coordinate transformation matrix with $l_1 = m_2 = \cos\theta$, $l_2 = -m_1 = \sin\theta$.

Hence, the averaged stress increments in the kth lamina can be determined from

$$\{d\sigma\}_k^G = ([T]_c)_k([S]_k)^{-1}([T]_c^T)_k\{d\epsilon\}_k^G \quad (13)$$

where

$$\{d\epsilon\}_k^G = \left\{ d\epsilon_{xx}^0 + \frac{z_k + z_{k-1}}{2} d\kappa_{xx}^0,\ d\epsilon_{yy}^0 + \frac{z_k + z_{k-1}}{2} d\kappa_{yy}^0, \right.$$

$$\left. 2d\epsilon_{xy}^0 + (z_k + z_{k-1})d\kappa_{xy}^0 \right\}^T \quad (14)$$

In Equation (14), z_k and z_{k-1} are the coordinates of the top and bottom surfaces of the lamina, respectively. These stresses are transformed into the local coordinates through

$$\{d\sigma\}_k = ([T]_s^T)_k\{d\sigma\}_k^G \quad (15)$$

where another coordinate transformation matrix, $[T]_s$, is defined as

$$[T]_s = \begin{bmatrix} l_1^2 & l_2^2 & l_1l_2 \\ m_1^2 & m_2^2 & m_1m_2 \\ 2l_1m_1 & 2l_2m_2 & l_1m_2 + l_2m_1 \end{bmatrix} \quad (16)$$

Substituting Equation (15) into the right-hand sides of Equations (1) and (2), the averaged stress increments in the fiber and matrix phases of this lamina can be calculated. It is thus necessary to determine only the middle surface strain and curvatures, defined in Equations (10.1) and (10.2). This can be achieved following the procedure of classical laminate analysis. The equations to determine these quantities thus obtained are [12]

$$\begin{Bmatrix} dN_{xx} \\ dN_{yy} \\ dN_{xy} \\ dM_{xx} \\ dM_{yy} \\ dM_{xy} \end{Bmatrix} = \begin{bmatrix} Q_{11}^{I} & Q_{12}^{I} & Q_{16}^{I} & Q_{11}^{II} & Q_{12}^{II} & Q_{16}^{II} \\ Q_{12}^{I} & Q_{22}^{I} & Q_{26}^{I} & Q_{12}^{II} & Q_{22}^{II} & Q_{26}^{II} \\ Q_{16}^{I} & Q_{26}^{I} & Q_{66}^{I} & Q_{16}^{II} & Q_{26}^{II} & Q_{66}^{II} \\ Q_{11}^{II} & Q_{12}^{II} & Q_{16}^{II} & Q_{11}^{III} & Q_{12}^{III} & Q_{16}^{III} \\ Q_{12}^{II} & Q_{22}^{II} & Q_{26}^{II} & Q_{12}^{III} & Q_{22}^{III} & Q_{26}^{III} \\ Q_{16}^{II} & Q_{26}^{II} & Q_{66}^{II} & Q_{16}^{III} & Q_{26}^{III} & Q_{66}^{III} \end{bmatrix} \begin{Bmatrix} d\epsilon_{xx}^{0} \\ d\epsilon_{yy}^{0} \\ 2d\epsilon_{xy}^{0} \\ d\kappa_{xx}^{0} \\ d\kappa_{yy}^{0} \\ 2d\kappa_{xy}^{0} \end{Bmatrix} \tag{17}$$

$$Q_{ij}^{I} = \sum_{k=1}^{N} (C_{ij}^{G})_k (z_k - z_{k-1}), \quad Q_{ij}^{II} = \frac{1}{2} \sum_{k=1}^{N} (C_{ij}^{G})_k (z_k^2 - z_{k-1}^2)$$

$$Q_{ij}^{III} = \frac{1}{3} \sum_{k=1}^{N} (C_{ij}^{G})_k (z_k^3 - z_{k-1}^3) \tag{18}$$

In Equation (18), N is the total number of lamina plies in the laminate, and $(C_{ij}^{G})_k$ are the stiffness elements of the kth lamina in the global system, see Equation (11). In Equation (17), dN_{xx}, dN_{yy}, dN_{xy}, dM_{xx}, dM_{yy}, and dM_{xy} are the overall incremental in-plane forces and moments per unit length exerted on the laminate, respectively. Supposing that the total applied in-plane stresses are $(\sigma_{xx}^{0}, \sigma_{yy}^{0}, \sigma_{xy}^{0})$, these forces and moments are defined as

$$dN_{xx} = \int_{-h/2}^{h/2} (d\sigma_{xx}^{0}) dz, \quad dN_{yy} = \int_{-h/2}^{h/2} (d\sigma_{yy}^{0}) dz, \quad dN_{xy} = \int_{-h/2}^{h/2} (d\sigma_{xy}^{0}) dz \tag{19.1}$$

$$dM_{xx} = \int_{-h/2}^{h/2} (d\sigma_{xx}^{0}) z dz, \quad dM_{yy} = \int_{-h/2}^{h/2} (d\sigma_{yy}^{0}) z dz, \quad dM_{xy} = \int_{-h/2}^{h/2} (d\sigma_{xy}^{0}) z dz \tag{19.2}$$

where

$$h = \sum_{k=1}^{N} (z_k - z_{k-1}) \tag{20}$$

is the total thickness of the laminate. If the in-plane stresses, $(\sigma^0_{xx}, \sigma^0_{yy}, \sigma^0_{xy})$, are evenly distributed on the laminate thickness with respect to the middle surface, the resulting moments from Equations (19.2) are all zero and no curvatures exist. The strain increments of all the laminae in the laminate will be the same. Even in such a case, however, the stress shared by each lamina in the laminate may be different due to a different ply-angle and/or compliance matrix. This can be seen clearly from Equation (13). Therefore, some lamina ply must have failed prior to others according to the strength criteria given in the previous section. As soon as one ply has failed, it no longer has any contribution to the overall instantaneous stiffness matrix of the laminate. The stress calculation of the remaining laminate plies will be carried out based on the overall stiffness matrix without the contribution from the failed lamina. More clearly, suppose that the k_0th lamina ply has failed. Then, for the next incremental load step, the middle surface strain and curvature increments are still calculated from Equations (17), but with different instantaneous overall stiffness elements, which are defined by

$$Q^I_{ij} = \sum_{\substack{k=1 \\ k\neq k_0}}^{N} (C^G_{ij})_k (z_k - z_{k-1}), \quad Q^{II}_{ij} = \frac{1}{2} \sum_{\substack{k=1 \\ k\neq k_0}}^{N} (C^G_{ij})_k (z_k^2 - z_{k-1}^2)$$

$$Q^{III}_{ij} = \frac{1}{3} \sum_{\substack{k=1 \\ k\neq k_0}}^{N} (C^G_{ij})_k (z_k^3 - z_{k-1}^3) \tag{21}$$

Note that the incremental forces and moments are determined using the same formulae, Equations (19.1) and (19.2). Continued in this way, the total failure strength of the laminate is determined using the overall applied load at which all the laminate plies have failed.

4. ANALYSIS PROCEDURE

In summation, the procedure for determining the total failure strength of the laminate can be expressed in the following steps. (For simplicity, suppose that all laminae have the same fiber and matrix properties and the same fiber volume fraction. Further, suppose that the fibers used are linearly elastic until rupture and the matrix is a bilinear elastic-plastic material.)

1. Input the constituent material properties: E_f, ν_f, $E^m, \nu^m, E^m_T, \sigma^m_Y, \sigma^f_u, \sigma^m_u, \sigma^f_{u,c}$, and $\sigma^m_{u,c}$, the fiber volume fraction: V_f, with $V_m = 1 - V_f$, ply number N, ply-angles: $\{\theta_k\}_{k=1}^N$, lamina surface coordinates: $\{z_k\}_{k=0}^N$; choose a power-index q (taken as 3 in this paper); calculate all the coordinate transformation

matrices: $\{([T]_c)_k\}_{k=1}^N$ and $\{([T]_s)_k\}_{k=1}^N$, according to Equations (12) and (16); define the initial bridging matrices: $\{[A]_k\}_{k=1}^N$, and the stiffness matrices: $\{[C]_k^G\}_{k=1}^N$, of all the laminae in the global system by using the linear elastic condition; calculate laminate overall stiffness elements Q_{ij}^I, Q_{ij}^{II}, and Q_{ij}^{III} from Equation (18); set k_0 = null and $N_0 = 0$.

2. For the given stress increments $(d\sigma_{xx}^0, d\sigma_{yy}^0, d\sigma_{xy}^0)$, calculate the in-plane force and moment increments, $\{dN\}=\{dN_{xx}, dN_{yy}, dN_{xy}\}^T$ and $\{dM\}=\{dM_{xx}, dM_{yy}, dM_{xy}\}^T$, from Equations (19.1) and (19.2).
3. Evaluate from Equation (17) the strain and curvature increments; calculate the stress increments exerted on each the kth but k_0th lamina: $\{d\sigma\}_k$, from Equations (13) and (15); further, evaluate from Equations (1) and (2) the internal stresses: $\{d\sigma^f\}_k$ and $\{d\sigma^m\}_k$, in the constituent phases of the lamina.
4. Update the total stresses through (initially zeros if there are no residual values):

$$\{\sigma\}^G=\{\sigma\}^G + \{d\sigma\}^G$$

$$\{\sigma^f\}_k = \{\sigma^f\}_k + \{d\sigma^f\}_k$$

$$\{\sigma^m\}_k = \{\sigma^m\}_k + \{d\sigma^m\}_k$$

check if there is a k_0, $1 \le k_0 \le N$, such that one of the internal stress states, $\{\sigma^f\}_{k_0}$ or $\{\sigma^m\}_{k_0}$, has reached its ultimate stress state (using the criteria given in Section 2); if so, $N_0 = N_0 + 1$, and the corresponding overall stress $\{\sigma\}^G$, is taken as the N_0-th failure stress state of the laminate.

5. If $N_0 = N$, stop calculation.
6. For every unfailed lamina k, $k \neq k_0$, evaluate the new compliance matrix: $([S^m])_k$, by using updated $\{\sigma^m\}_k$; define the new bridging matrices: $([A])_k$, by means of Equations (5) and (6) and calculate the compliance matrix $([S])_k$ from Equation (3); evaluate the global stiffness matrix of the lamina: $[C]_k^G$, see Equation (11); determine the overall stiffness elements Q_{ij}^I, Q_{ij}^{II}, and Q_{ij}^{III} from Equation (21); go to (2).

5. APPLICATION EXAMPLES

Four different glass-fiber-reinforced epoxy-matrix angle-ply laminates subjected to various combined biaxial loads are simulated using the analysis procedure described in the previous section. The predicted failure envelopes of these laminates are compared with available experimental data.

The first angle-ply laminate, $[\pm 30°]_s$, is a $\pm 30°$ helical winding shell made using glass fibers and an epoxy matrix, subjected to combined axial (normal stress) and torsion (in-plane shear stress) loads. The axial direction of the shell is taken as the

global x-coordinate, while its circumferential direction is taken as the y-coordinate. The ultimate failure envelope of this composite under different combinations of axial normal and in-plane shear stresses was measured by Krauss and Schelling [13]. Their results are used as a comparison and are shown in Figure 1. The given material parameters are [14]: $E_f = 70$ GPa, $\nu_f = 0.23$, $E_m = 3.5$ GPa, $\nu_m = 0.35$, and $\sigma_u^m = 70$ MPa, with a fiber volume fraction of $V_f = 0.63$. The tensile strength of the fiber, $\sigma_u^f = 2150$ MPa, is taken from Reference [15], whereas the compressive strengths of the fiber and the matrix are considered as equal to their tensile strengths. As no plasticity information for the epoxy used is available, this epoxy matrix is simply assumed to be linearly elastic until rupture in the present calculation. The predicted first-ply and last-ply failure envelopes are plotted in Figure 1. Due to symmetry, only the upper halves of the envelopes are plotted. The first-ply failure is initiated from the matrix fracture. Hence, the first ply must be the ply for which the principal stress in the matrix due to the in-plane shear has a smaller inclined angle with the axial direction. It is seen that correlation between the predicted and measured ultimate failure curves is fair. The correlation can be improved if the matrix undergoes some plastic deformation and if the compressive strength of the matrix is adjusted to some lower value, as can be seen from the following examples.

The remaining examples are taken from Reference [16]. They are angle-ply laminates with ply-angles of ±45°, ±55°, and ±75°. The experimental work for these composites has been done by Soden et al. [16], who measured the final fail-

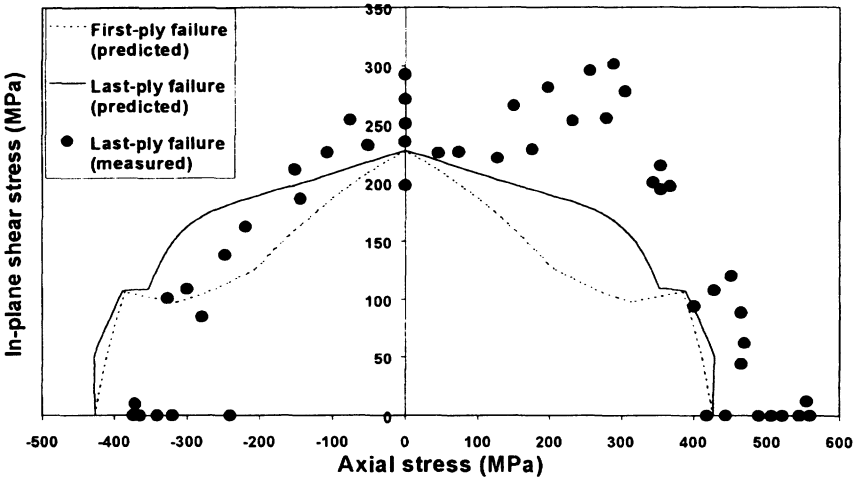

Figure 1. *Predicted and measured [13] failure envelopes of a ±30° ply glass/epoxy laminate subjected to combined axial tension and torsion loads. The parameters used are* $E_f = 70$ *GPa,* $\nu_f = 0.23$, $\sigma_u^f = \sigma_{u,c}^f = 2150$ *MPa,* $E^m = 3.5$ *GPa,* $\nu_m = 0.35$, $\sigma_Y^m = \sigma_u^m = \sigma_{u,c}^m$ *70 MPa, and* $V_f = 0.63$.

ure envelopes of the shells subjected to biaxial tensions, i.e., tensile loads in the x- and y-directions. Different biaxial tensions were achieved through adjusting internal pressures and axial loads. The E-glass fiber reinforcement was Silenka 051L, 1200 tex, and the epoxy resin system was Ciba-Geigy MY750/HY917/DY063. Properties of these constituent materials have been reported in Reference [15]: E_f = 74 GPa, $\nu_f = 0.22$, $\sigma_u^f = 2150$ MPa, $\sigma_{u,c}^f = 1450$ MPa, $E^m = 3.35$ GPa, $\nu^m = 0.35$, $\sigma_u^m = 80$ MPa, $\sigma_{u,c}^m = 120$ MPa, and $\epsilon_u^m = 5\%$, where ϵ_u^m is the ultimate strain of the matrix. Hence, the matrix used displays an inelastic deformation before failure. In the present analysis, a bilinear elasto-plastic behavior is assumed. Taking a yield strength as $\sigma_Y^m = 50$ MPa, the matrix hardening modulus is found to be $E_T^m = 850$ MPa. Using these parameters, the predicted failure envelopes for the laminates $[\pm 45°]_s$, $[\pm 55°]_s$, and $[\pm 75°]_s$ are plotted in Figures 2 through 4, respectively. The experimental data by Soden et al. [16] are also shown in the corresponding figures. From these figures, it is seen that the best correlation between the prediction and the experimental results is for the laminate $[\pm 55°]_s$ shown in Figure 3, in which the predicted failure envelope agrees fairly well with the measured data. For the other two laminates, discrepancy exists between some parts of the predicted envelopes and the corresponding experimental data.

For the laminate $[\pm 45°]_s$, almost half of the predicted tensile failure curve, which is above the horizontal axis (hoop stress axis), correlates very well with the measured data. The remaining half of the tensile curve, however, has some dis-

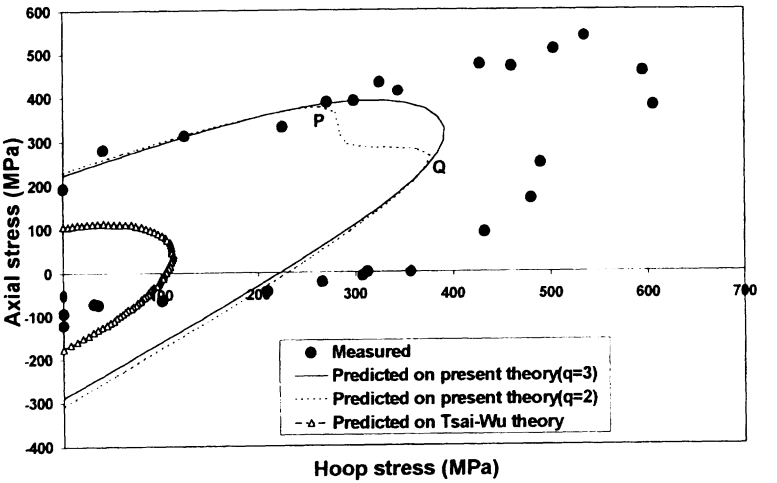

Figure 2. *Predicted and measured [16] failure envelopes of a ±45° helical glass/epoxy shell subjected to combined axial and circumferential tensile loads. The parameters used are* E_f = *74 GPa,* ν_f = *0.22,* σ_u^f = *2150 MPa,* $\sigma_{u,c}^f$ = *1450 MPa,* E^m = *3.35 GPa,* ν^m = *0.35,* σ_Y^m = *50 MPa,* E_T^m = *850 MPa,* σ_u^m = *80 MPa,* $\sigma_{u,c}^m$ = *120 MPa, and* V_f = *0.504.*

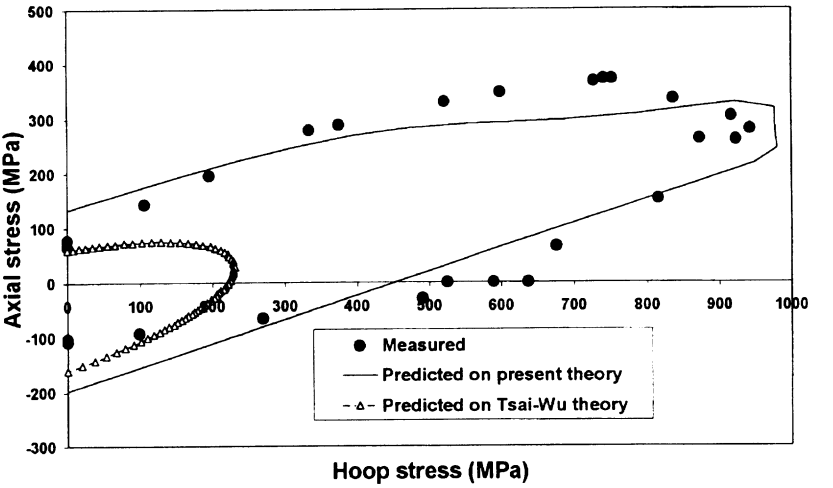

Figure 3. *Predicted and measured [16] failure envelopes of a ±55° helical glass/epoxy shell subjected to combined axial and circumferential tensile loads. The parameters used are the same as those in Figure 2 except* V_f, which is 0.602 in this composite.

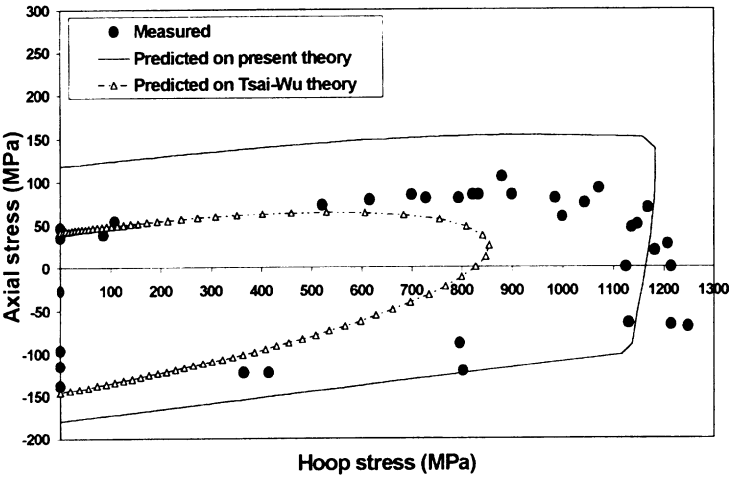

Figure 4. *Predicted and measured [16] failure envelopes of a ±75° helical glass/epoxy shell subjected to combined axial and circumferential tensile loads. The parameters used are the same as those in Figure 2 except* V_f, *which is 0.567 in this composite.*

crepancy with the experiments. It should be pointed out that the predicted tensile failure curve is completely symmetric with respect to a stress line $\sigma_{xx} = \sigma_{yy}$, as the laminate, $[\pm 45°]_s$, is a quasi-isotropic material and is subjected to symmetric tensile loads along the two material principal axes, x and y. On the other hand, the measured data do not show a perfect symmetry. The other half of the experimental tensile data seems to have some shift from the symmetrical axis.

When the composite is subjected to compressive loads, the predicted failure curve differs from the measured data significantly. This may be attributed to an inaccurate measurement for the laminate compressive strengths, or an incorrect usage of the matrix compressive strength in the prediction. From Figure 2, one can clearly see that the measured compressive strengths of the composite are significantly lower than the corresponding tensile strengths. Intuitively, under such low compressive loads and if no material buckling is involved, the failure of the composite should most probably result from the matrix fracture. This is precisely the failure mode of the present prediction. However, as an even higher matrix compressive strength (as high as 1.5 times the tensile strength) has been used, the predicted compressive failure strength of the composite in the axial direction is thus higher than the predicted tensile failure strength.

In order to gain some idea about the influence of the power-index q chosen in Equation (8.2) on the prediction, another trial with $q = 2$ was carried out; the results are also plotted in Figure 2. The figure suggests that this index should be taken as $q > 2$, since with $q = 2$ the predicted curve segment, PQ, has a concave shape and also differs more from the experiment. On the other hand, the majority of the predicted failure curves almost coincide with each other regardless of any power-index used. This means that the maximum normal stress criterion is able to meet most load combinations.

For the laminate $[\pm 75°]_s$, the lower part of the predicted curve (below the horizontal axis) correlates fairly well with the experiment; see Figure 4. The largest difference between the prediction and the experiment occurs when the laminate is subjected to uniaxial tension (i.e., hoop stress = 0). Under this load condition, the predicted failure strength is 118 MPa, whereas the measured value is around 45 MPa only. Recognizing that the matrix ultimate tensile strength is 80 MPa, there must be some unseen reasons involved. Phenomenologically, if there are no fabrication defects and no residual thermal stresses in any of the constituent fiber and matrix materials, the resulting composite strength in any direction should not be lower than that of either constituent. Therefore, the low measured strength, 45 MPa, might be attributed to residual thermal stresses already existing in the constituents before testing, sample defects, measurement error, or reduction in the matrix strength after fabrication.

To better understand the efficiency of the present theory, predictions for the failure envelopes of the last three laminates using another popular theory, the Tsai-Wu theory [17], have also been made and are plotted in Figures 2–4 for comparison.

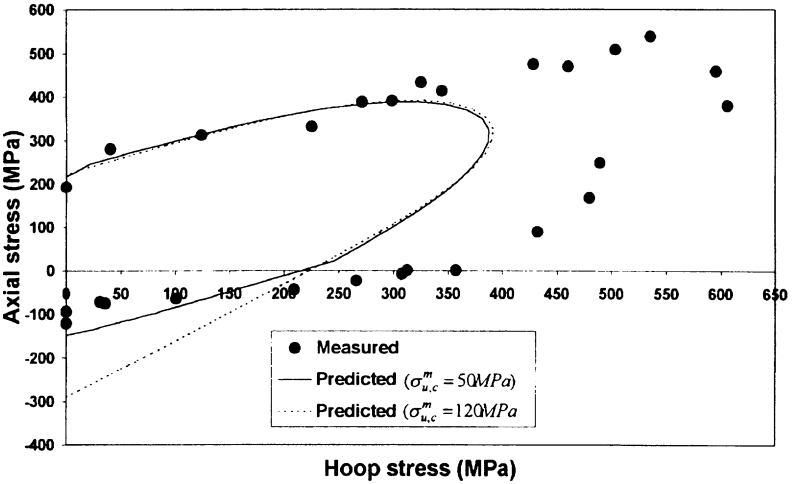

Figure 5. *Predicted and measured [16] failure envelopes of a ±45° helical glass/epoxy shell subjected to combined axial and circumferential tensile loads. The parameters used are* E_f = *74 GPa,* ν_f = *0.22,* σ^f_u = *2150 MPa,* $\sigma^f_{u,c}$ = *1450 MPa,* E^m = *3.35 GPa,* ν^m = *0.35,* σ^m_Y = *50 MPa,* E^m_T = *850 MPa,* σ^m_u = *80 MPa, and* V_f = *0.504.*

The unidirectional lamina strengths, which were used to determine the strength parameters involved in the Tsai-Wu theory, had been taken from Reference [15]. They are, respectively, the longitudinal tensile and compressive strengths $X = 1280$ MPa and $X' = 800$ MPa, the transverse tensile and compressive strengths $Y = 40$ MPa and $Y' = 145$ MPa, and the shear strength $S = 73$ MPa. As usual, no matrix plasticity was assumed during the predictions when applying the Tsai-Wu theory. It can be seen that as a whole the predicted failure envelopes based on the present theory agree better with the experiments than those based on the Tsai-Wu theory. Further, all the predictions with the present theory used only the original material data, i.e., material properties tested using samples of neat (pure) matrix and fibers. However, some calibrations of material parameters using some test results of the composites under consideration would be beneficial for a better prediction, as indicated in Figure 5 for the $[\pm 45°]_s$ laminate. In Figure 5, all the other parameters used are the same as those in Figure 2 except that different matrix compressive strengths were employed. The compressive strength $\sigma^m_{u,c} = 50$ MPa gave much better prediction for the lower part of the envelope than the strength $\sigma^m_{u,c} = 120$ MPa. The other part of the predictions based on these two strengths coincide with each other. This is because the other part of the failure envelope is not controlled by the matrix compressive strength. Considering the fact that large deviations are generally observed in the measurement of laminate strength behavior, the present prediction can be regarded as reasonable.

CONCLUSION

Using the unified micromechanical model developed in References [1], [2], and [3], and the classical laminate theory, the progressive failure process in a laminated composite can be easily simulated. This has been done in the present paper. The simulation employs minimal experimental data, which can be obtained through simple tensile and compressive tests on the constituent fiber and matrix materials of the laminate. If not available, they can be inversely determined using the ultimate longitudinal and transverse tensile and compressive strengths of a unidirectional lamina constituting the laminate, as has been shown in Reference [3]. Neither biaxial tensile/compressive testing nor shear testing is required. Four different angle-ply laminates subjected to various biaxial loads have been analyzed. The predicted failure envelopes, using neat material properties without any calibration, are in reasonable agreement with the available experimental data.

REFERENCES

1. Huang, Z. M., "A Unified Micromechanical Model for the Mechanical Properties of Two Constituent Composite Materials. Part I: Elastic Behavior," *J. Thermoplastic Composite Materials* (in press).
2. Huang, Z. M., "A Unified Micromechanical Model for the Mechanical Properties of Two Constituent Composite Materials. Part II: Plastic Behavior," *J. Thermoplastic Composite Materials* (in press).
3. Huang, Z. M., "A Unified Micromechanical Model for the Mechanical Properties of Two Constituent Composite Materials. Part III: Strength Behavior," *J. Thermoplastic Composite Materials* (in press).
4. Huang, Z. M., "A Unified Micromechanical Model for the Mechanical Properties of Two Constituent Composite Materials. Part IV: Rubber-Elastic Behavior," *J. Thermoplastic Composite Materials* (in press).
5. Soni, S. R., 1983, "A Comparative Study of Failure Envelopes in Composite Laminate," *J. Reinf. Plast. Compos.*, Vol. 2, pp. 34–42.
6. Tsai, S. W., 1984, "A Survey of Macroscopic Failure Criteria for Composite Materials," Vol. 3, pp. 40–62.
7. Rowlands, R. E., 1985, "Strength (Failure) Theories and Their Experimental Correlation," in G. C. Sih & A. M. Skudra eds., *Failure Mechanics of Composites*, Handbook of Composites, Vol. 3, North-Holland, New York, pp. 71–128.
8. Nahas, M. N., 1986, "Survey of Failure and Post-Failure Theories of Laminated Fiber-Reinforced Composites," *J. Comp. Tech. & Res.*, Vol. 8, No. 4, pp. 138–153.
9. Echaabi, J., Trochu, F., & Gauvin, R., 1996, "Review of Failure Criteria of Fibrous Composite Materials," *Poly. Comp.*, Vol. 17, No. 6, pp. 786–798.
10. Hinton, M. J. and Soden, P. D., 1998," Predicting Failure in Composite Laminates: The Background to the Exercise," *Comp. Sci. & Tech.*, Vol. 58, pp. 1001–1010.
11. Soden, P. D., Hinton, M. J., and Kaddour, A. S., 1998, "A Comparison of the Predictive Capabilities of Current Failure Theories for Composite Laminates," *Comp. Sci. & Tech.*, Vol. 58, pp. 1225–1254.
12. Gibson, R. F., 1994, *Principles of Composite Material Mechanics*, McGraw-Hill, Inc., New York, pp. 201–207.

13. Krauss, H. and Schelling, H., 1969, *Kunststoffe*, Vol. 59, Chapter 12, p. 911.
14. Skudra, A. M., 1985, "Micromechanics of Failure of Reinforced Plastics," in G. C. Sih & A. M. Skudra eds., *Failure Mechanics of Composites, Handbook of Composites,* Vol. 3, North-Holland, New York, pp. 1–69.
15. Soden, P. D., Hinton, M. J., & Kaddour, A. S., 1998, "Lamina Properties, Lay-up Configurations and Loading Conditions for a Range of Fiber-Reinforced Composite Laminates," *Comp. Sci. & Tech*, Vol. 58, pp. 1011–1022.
16. Soden, P. D., Kitching, R., Tse, P. C., Tsavalas, Y., and Hinton, M. J., 1993, "Influence of Winding Angle of the Strength and Deformation of Filament-Wound Composite Tubes Subjected to Uniaxial and Biaxial Loads," *Comp. Sci. & Tech.*, Vol. 46, pp. 363–378.
17. Tsai, S. W. & Hahn, H. T., 1980, *Introduction to Composite Materials*, Technomic Publishing Co., Inc., Lancaster.